

# JGR Solid Earth

## RESEARCH ARTICLE

10.1029/2020JB019739

### Key Points:

- Great Lakes water levels rose 0.7–1.5 m from 2013 to 2019, causing the lake floor and adjacent land to fall 3–23 mm
- Seasonal water storage on land in the Great Lakes watershed is inferred to be maximum in March and twice as big as in a hydrology model
- Groundwater in the Great Lakes watershed has a peak-to-peak seasonal oscillation of 60 km<sup>3</sup> and remained nearly constant from 2004 to 2019

### Supporting Information:

- Supporting Information S1

### Correspondence to:

D. F. Argus,  
donald.f.argus@jpl.nasa.gov

### Citation:

Argus, D. F., Ratliff, B., DeMets, C., Borsa, A. A., Wiese, D. N., & Blewitt, G., et al. (2020). Rise of Great Lakes surface water, sinking of the upper Midwest of the United States, and viscous collapse of the forebulge of the former Laurentide ice sheet. *Journal of Geophysical Research: Solid Earth*, 125, e2020JB019739. <https://doi.org/10.1029/2020JB019739>

Received 13 MAR 2020

Accepted 25 JUL 2020

Accepted article online 31 JUL 2020

## Rise of Great Lakes Surface Water, Sinking of the Upper Midwest of the United States, and Viscous Collapse of the Forebulge of the Former Laurentide Ice Sheet

Donald F. Argus<sup>1</sup> , Benjamin Ratliff<sup>2</sup>, Charles DeMets<sup>2</sup> , Adrian A. Borsa<sup>3</sup> , David N. Wiese<sup>1</sup> , Geoffrey Blewitt<sup>4</sup> , John W. Crowley<sup>5</sup> , Hilary R. Martens<sup>6</sup> , Corné Kreemer<sup>4</sup> , and Felix W. Landerer<sup>1</sup> 

<sup>1</sup>Jet Propulsion Laboratory, California Institute of Technology, Pasadena, CA, USA, <sup>2</sup>Department of Geoscience, University of Wisconsin-Madison, Madison, WI, USA, <sup>3</sup>Scripps Institution of Oceanography, University of California, San Diego, La Jolla, CA, USA, <sup>4</sup>Nevada Geodetic Laboratory, Nevada Bureau of Mines and Geology, University of Nevada, Reno, Reno, NV, USA, <sup>5</sup>Canadian Geodetic Survey, National Resources Canada, Ottawa, Ontario, Canada, <sup>6</sup>Department of Geosciences, University of Montana, Missoula, MT, USA

**Abstract** Great Lakes water levels rose 0.7–1.5 m from 2013 to 2019, increasing surface water volume by 285 km<sup>3</sup>. Solid Earth's elastic response to the increased mass load is nearly known: The Great Lakes floor fell 8–23 mm, and the adjacent land fell 3–14 mm. Correcting GPS measurements for this predicted elastic loading (1) straightens position-time series, making the evolution of position more nearly a constant velocity and (2) reduces estimates of subsidence rate in Wisconsin, Michigan, and southern Ontario by 0.5–2 mm/yr, improving constraints on postglacial rebound. GPS records Wisconsin and Michigan to have subsided at 1–4 mm/yr. We find this sinking to be produced primarily by viscous collapse of the former Laurentide ice sheet forebulge and secondarily by elastic Great Lakes loading. We infer water on land in the Great Lakes watershed to be total water change observed by GRACE minus Great Lakes surface water smeared by a Gaussian distribution. Water stored on land each year reaches a maximum in March, 6 months before Great Lakes water levels peak in September. The seasonal oscillation of water on land in the Great Lakes basin, 100 km<sup>3</sup> (0.20 m water thickness), is twice that in a hydrology model. In the seasons, groundwater in the Great Lakes watershed increases by 60 km<sup>3</sup> (0.12 m) each autumn and winter and decreases by roughly an equivalent amount each spring and summer. In the long term, groundwater volume remained constant from 2004 to 2012 but increased by 50 km<sup>3</sup> (0.10 m) from 2013 to 2019.

## 1. Introduction

Measurements of change in total water storage from space are providing strong constraints on mass transfer in water cycle processes. GRACE gravity data from 2002 to 2019 determine changes in continental water storage to an accuracy of about 0.02 m over distances 400 km in dimension (Dahle et al., 2019; Luthcke et al., 2013; Save et al., 2016; Watkins et al., 2015). GRACE brings insight to the relationship between water storage, river discharge, and flooding in the United States (Reager et al., 2014) and suggests that hydrology models underestimate long-term change in total water (Scanlon et al., 2018).

GPS positioning is emerging as a second effective technique to infer change in total water storage. Solid Earth's elastic displacement to change in mass is approximately known for surface loads more than 50 km across. GPS vertical displacements have been inverted to infer changes in water at Earth's surface as a function of time (Argus et al., 2014; Borsa et al., 2014; Fu et al., 2015). In places with a dense spacing of GPS sites, such as California, Oregon, and Washington, change in total water has been inferred at a spatial resolution of 75 km, thus improving the spatial resolution of the GRACE determination of mass change.

Argus et al. (2017) quantify mass transfer in water cycle processes using GPS inferences of water change. In California's mountains, Argus et al. (2017) find more water in the ground to be lost during periods of drought and gained in years of heavy precipitation than in hydrology models. By integrating GPS estimates of water change with a hydrology model, Argus et al. (2017) infer substantial snowmelt to infiltrate the ground each spring and significant water to be parched from the ground each summer and autumn. Argus et al. (2017) conclude that the ground has a greater capacity to store water than previously believed, a conclusion

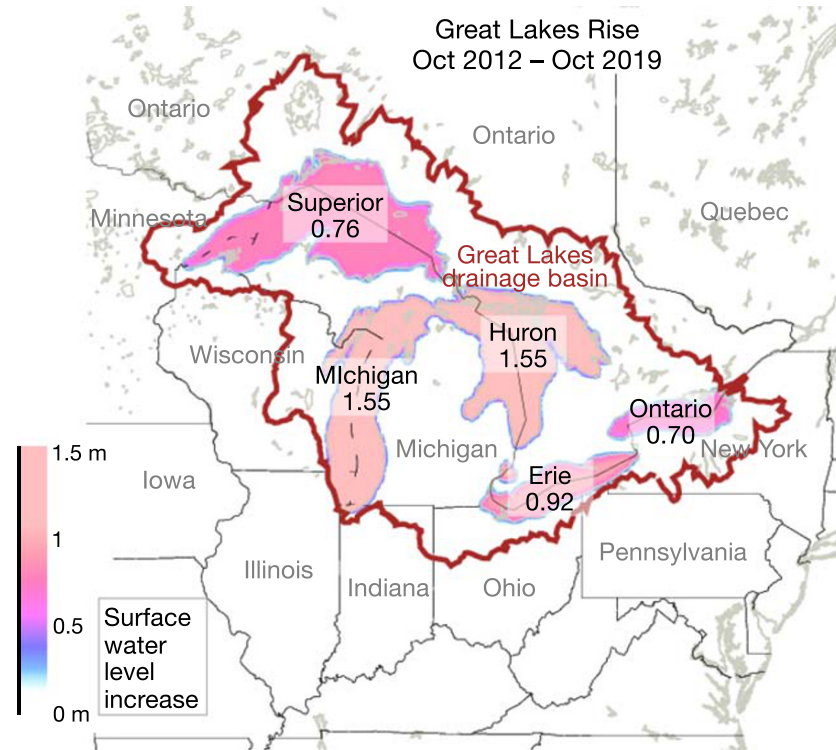


**Figure 1.** Rise in surface water level (in meters) in the five Great Lakes from October 2012 to October 2019 measured by water level gauges. The Great Lake drainage basin (brown outline) is defined by all rivers flowing into the Great Lakes.

supported by Enzminger et al.'s (2019) finding of significant fluctuations in subsurface water storage in the Sierra Nevada mountains, California.

In an interdisciplinary NASA endeavor crosscutting between solid Earth science and hydrology, we are integrating GPS measurements of elastic land displacements and GRACE gravity observations to infer change in water at Earth's surface (e.g., Adusumilli et al., 2019). We aim to strengthen and sharpen GRACE's image of change in total water by rigorously adding GPS constraints in places with a dense spacing of GPS sites. In Michigan, Wisconsin, and southern Ontario, changes in Great Lakes surface water are greater than changes in water on land in the Great Lakes drainage basin. In this study, we therefore first remove the elastic signature of changes in Great Lakes surface water from the GRACE and GPS measurements and next remove the solid Earth's viscous response to unloading of the late Pleistocene ice sheets from the GPS data (glacial isostatic adjustment is already removed from the GRACE data). We then evaluate the remaining GPS and GRACE signals as changes in water on land in the Great Lakes watershed. This study advances understanding of a range of solid Earth and water cycle phenomena.

## 2. Data and Methods

### 2.1. GPS

Position-time series of 3,658 GPS sites from 1994 to 2019 are determined by scientists at the Nevada Geodetic Laboratory (NGL) (Blewitt et al., 2018, 2019). Position as a function of time at 18,414 worldwide GPS sites are determined in the IGS14 reference frame (Reischung et al., 2016) as part of a complete reanalysis (Blewitt et al., 2019) using Jet Propulsion Laboratory (JPL)'s satellite orbits and clocks. Atmospheric loading is removed using European Centre for Medium-Range Weather Forecasts (ECMWF) (Dill & Dobslaw, 2013). Each GPS position-time series is fit with a position, a velocity, a sinusoid with a period of 1 yr, and offsets at the time of logged antenna substitutions following the methods of Argus et al. (2010). Please see the supporting information for a full description of the advanced GPS positioning techniques.

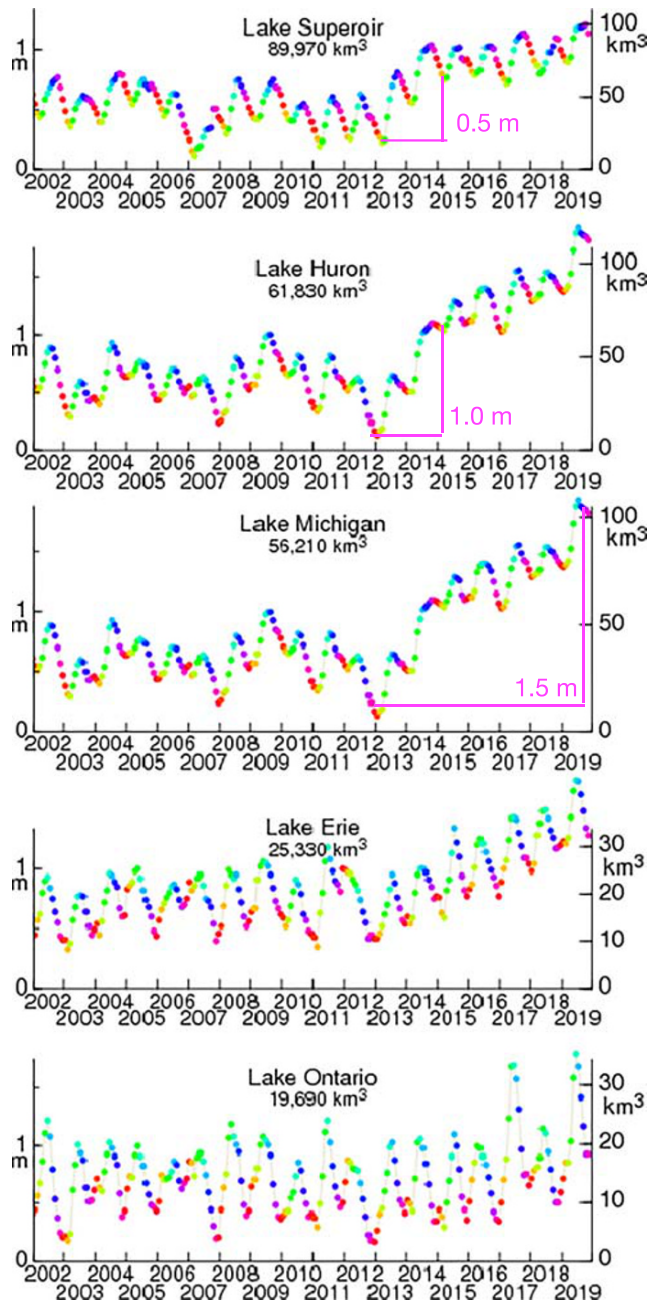


**Figure 2.** Change in water levels in the five Great Lakes from January 2002 to December 2019 measured by water level gauges (dots with different colors signify the seasons). Lake Superior rose 0.5 m in 2013 and 2014. Lake Huron and Lake Michigan, at the same water level, rose 1 m in 2013 and 2014 and rose 1.5 m from 2013 to 2019 (magenta line segments). Vertical axes at left are in meters and identical; vertical axes at right are in cubic kilometers and depend on Great Lake area. See Figure S1 for change in Great Lakes surface water level from 1991 to 2019.

## 2.2. GRACE

Time series of change in total water storage at Earth's surface from 2002 to 2019 are determined by scientists at JPL (Watkins et al., 2015; Wiese et al., 2016). In the mass concentration (“mascon”) solution, changes in total water in  $3^\circ \times 3^\circ$  spherical caps are estimated directly from satellite-to-satellite range-rate (“K-band”) data. A “mascon” solution (see also Luthcke et al., 2013; Save et al., 2016) is less subject to leakage of gravity signal outside a specific place than a spherical harmonic solution. A regularization constraint is enforced in space and time to reduce correlated errors, such as anomalous north-south stripes. GRACE measurements of gravity change are corrected for glacial isostatic adjustment (model ICE-6G\_D (VM5a)). The GRACE estimates of water change in this study are therefore primarily fluctuations in water, snow, ice, and atmosphere.

## 2.3. Composite Hydrology Model

In this study, we compare against a composite hydrology model consisting of snow water equivalent in Snow Data Assimilation System (SNODAS) and soil moisture in North American Global Land Assimilations System (NLDAS)-Noah. The NLDAS (Mitchell et al., 2004) specifies snow water equivalent and soil moisture each month at  $(1/8)^\circ$  intervals of latitude and longitude. Land surface models such as NLDAS in general do not include either groundwater or surface water. The SNODAS (National Operational Hydrologic Remote Sensing Center, 2004; National Snow and Ice Data Center, 2019) specifies snow water equivalent each day at 1 km intervals. Snow Telemetry (SNOTEL) measurements suggest snow water equivalent is about 4 times greater than in NLDAS-Noah (Pan et al., 2003). Therefore, our composite hydrology model is based on SNODAS, which incorporates the SNOTEL data.

## 3. Results

### 3.1. Rise of Water Level in the Great Lakes

The water level of each of the five Great Lakes is accurately determined by the Coordinating Committee on Great Lakes Basic Hydraulic and Hydrologic Data (Gronewold et al., 2013, 2018) using 21 gauging stations (Figures 1 and 2). Five water level gauges are along the coast of Lake Superior, six are along Lake Michigan and Lake Huron (which are connected and at the same water level), four are along Lake Erie, and six are along Lake Ontario. The measured water level each month is available from the U.S. Army Corps of Engineers (at [http://lre-wm.usace.army.mil/ForecastData/GLHYD\\_data\\_metric.csv](http://lre-wm.usace.army.mil/ForecastData/GLHYD_data_metric.csv)). Satellite altimetry estimates of the water height of the five Great Lakes relative to Earth's mass center (CM) confirm that the water level gauge measurements are correct (Jia et al., 2018) (Figure S1). Satellite altimetry measurements of the height of the Great Lakes are provided by the U.S. Department of Agriculture/NASA Global Reservoir and Lake Elevations Database (G-REALM) project (at [https://ipad.fas.usda.gov/cropexplorer/global\\_reservoir/](https://ipad.fas.usda.gov/cropexplorer/global_reservoir/)).

Water levels in the Great Lakes rose dramatically from October 2012 to October 2019, increasing surface water volume by  $285 \text{ km}^3$ . In total, Lake Superior rose 0.76 m, Lake Huron and Lake Michigan rose 1.55 m, Lake Erie rose 0.92 m, and Lake Ontario rose 0.70 m from 2013 to 2019 (Figure 1). Water levels

rose the most in 2013 and 2014, with Superior rising 0.5 m and Huron and Michigan rising 1 m (Figure 2). The Great Lakes abrupt rise in 2013 and 2014 coincided with cold weather when extensive ice covered the Great Lakes (Gronewold et al., 2016). In 2013, Lakes Superior, Michigan, and Huron rose in response to increased spring runoff and high precipitation over the lakes. In 2014, a combination of low evaporation, increased runoff, and water flow from Lake Superior caused Huron, Michigan, and Superior to rise. Water levels in Lake Huron and Lake Michigan rose slowly from 2015 to 2018 but quickly in 2019.

From 1997 to 2000, water levels in the Great Lakes fell, reducing surface water volume by 200 km<sup>3</sup> (Figure S1). Lake Superior fell 0.5 m, and Lake Michigan and Lake Huron each fell 1.0 m. Kling et al. (2003) and Dempsey et al. (2008) explore the ecological and infrastructural damage from this Great Lakes water decrease in the context of global climate change.

Water levels in the Great Lakes furthermore oscillate in the seasons. Each year, water levels rise about 0.3 m in the spring and summer as melting snow moves through rivers into the Great Lakes, and water levels fall roughly an equivalent amount in the autumn and winter when evaporation is low and when snow accumulates on land. Water on land in the Great Lakes drainage basin, consisting of snow and soil moisture in a hydrology model, is maximum in March, 6 months before Great Lakes surface water is maximum in September.

Change in water levels differ slightly between the northern and southern shores of each connected Great Lake by an amount of roughly 1% of the total change in water level. Using water level gauge data from 1860 to 2000, Mainville and Craymer (2005) find the water level at Parry Sound (PARR), along the northeast shore of Lake Huron, fell 3.4 mm/yr faster than Calumet City (CALU), at the southern tip of Lake Michigan. The ICE-6G\_D (VM5a) postglacial rebound model predicts Earth's surface at PARR to be rising at 1.7 mm/yr and at CALU to be subsiding at 1.6 mm/yr, yielding a relative rate of vertical land motion (3.3 mm/yr) that explains the difference in water level rates (see also Roy & Peltier, 2017, Figure 5).

### 3.2. Solid Earth's Elastic Response to Increased Great Lakes Surface Water

Solid Earth's elastic response to changes in surface mass load is approximately known (Argus et al., 2017; Wahr et al., 2013). Earth's elastic response is not very sensitive to Earth's rheologic structure for loads greater than 50 km in dimension. For example, the Gutenberg-Bullen A Earth model (Farrell, 1972) and the Preliminary Earth Reference Model (PREM) (Wang et al., 2012) produce nearly identical elastic displacement in response to a mass load (Argus et al., 2017, Figure S1).

We calculate solid Earth's elastic response to changes in Great Lakes surface water volume as measured with water level gauges as follows. We take the density of the freshwater in the Great Lakes to be 1,000 kg/m<sup>3</sup>. We assume solid Earth's elastic response to be given by Green's functions (Wang et al., 2012) for a gravitating, spherical, stratified Earth with the PREM Earth structure (Dziewonski & Anderson, 1981). Following Argus et al. (2017), we numerically integrate the Green's functions to attain modified (Green's) functions specifying solid Earth's elastic response to a disk with a specific radius. We then calculate solid Earth's elastic response to the sum of changes in surface water measured by water level gauges each month at 118,389 elements inside the five Great Lakes at (1/64)<sup>o</sup> intervals of latitude and longitude.

The elastic response we calculate in this manner is nearly identical to that calculated from SPOTL (Agnew, 2013) and from LoadDef (Martens et al., 2019). The elastic response in this study is furthermore identical to that used to correct GRACE gravity estimates of change in equivalent water thickness for solid Earth's elastic response to changes in the mass load (Save et al., 2016; Watkins et al., 2015). It is essential to calculate solid Earth's elastic response on a gravitating sphere. Nongravitating, half-space calculations (e.g., D'Urso & Marmo, 2013) overstate solid Earth's elastic response by a factor of 2.5 (Argus et al., 2017, Figure S20).

From October 2012 to October 2019, as the Great Lakes rose 0.7–1.5 m, the floor of the Great Lakes fell 8–23 mm, and the adjacent land in Michigan, Wisconsin, southern Ontario, Illinois, Indiana, and Ohio fell 3–14 mm (Figure 3; see also Figure S4). The amount of subsidence decreases with distance from the Great Lakes from its maximum of 23 mm beneath Lake Huron to 3 mm at places 100–200 km from the Great Lakes. The increased load of the Lakes also caused the adjacent area to move horizontally 1–4 mm toward the Great Lakes, with maximum inward displacements at LCUR (3.9 mm) and PARR (3.9 mm) (Figure S2).

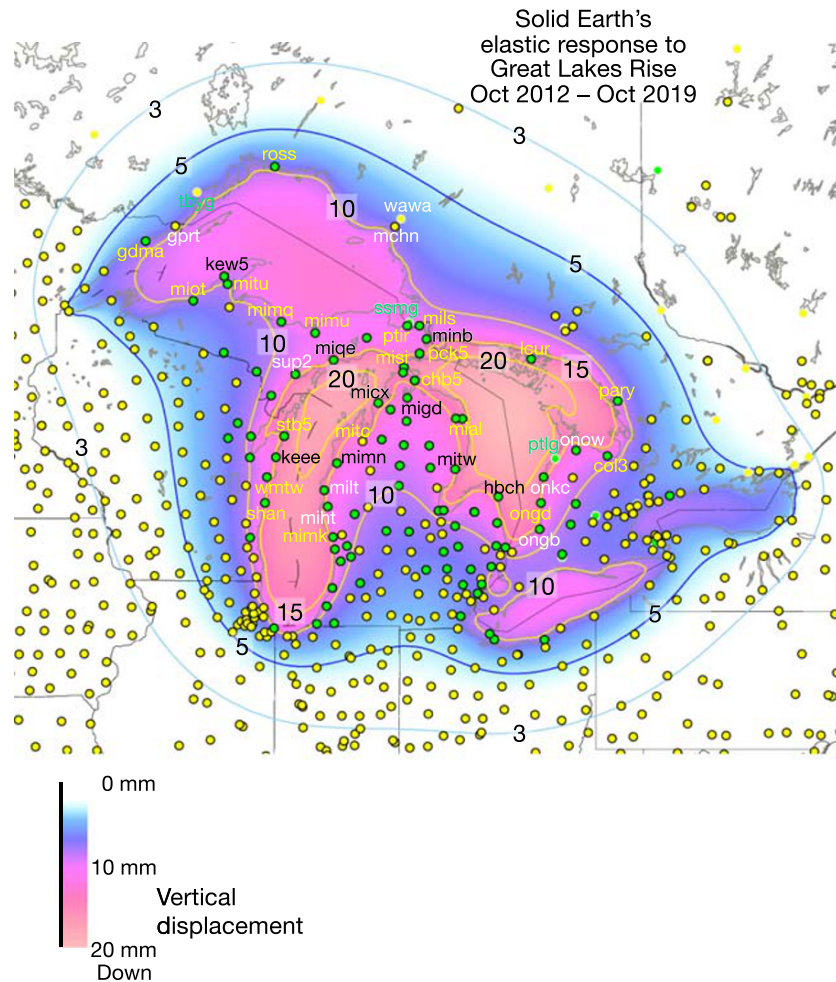


**Figure 3.** Solid Earth's subsidence (blue to magenta color gradations) in elastic response to the increase in Great Lakes surface water from October 2012 to October 2019. Contours are at 3, 5, 10, 15, and 20 mm of subsidence. The floor of the Great Lakes fell 8–23 mm. Earth's surface in Michigan, Wisconsin, and southernmost Ontario fell 3–15 mm. A total of 104 GPS sites have more than a 25% reduction in dispersion in vertical position when elastic Great Lakes loading is corrected for (circles filled green); the remaining GPS sites have less than a 25% reduction (circles filled yellow). Most GPS sites have continuous data (black circle outline); campaign GPS sites from the Canadian Base Network have observations roughly every 5 years (no black circle outline). The four-letter abbreviations of the 10 GPS sites in Figure 4 are in black text. The four-letter abbreviations of the GPS sites in Figures S5–S7 are in yellow.

The floor at the center of Lake Huron fell 23 mm from October 2012 to October 2019, more than the 10 mm fall of the Lake Superior coast. The subsidence of the deep Lakes floor caused relative sea level at the gauging stations to fall about 10 mm, just 1% of the total rise of the Great Lakes of roughly 1 m. We do not adjust for this very small effect on gauging measurement of lake levels.

### 3.3. Correcting GPS Series for Great Lakes Surface Water Elastic Loading

As we would expect, correcting time series of GPS site positions near the Great Lakes for elastic surface water loading straightens the evolution of position with time, making the series more nearly a constant velocity (Figures 4 and S5–S7). At 91 GPS sites near the Great Lakes, correcting for elastic loading of surface water reduces the root-mean-square (rms) dispersion of the monthly mean of the vertical component of position by 26% to 51%. The dispersion reduction is greatest where the elastic response to Great Lakes surface water is greatest—along the west coast of Lake Huron, east coast of Lake Michigan, and near the intersection of Lakes Superior, Huron, and Michigan. The rms misfit of GPS estimates of vertical position at (HBCH) Harbor Beach, Michigan, decreases by 51% (from 4.1 mm to 2.0 mm). The rms misfit of mean monthly

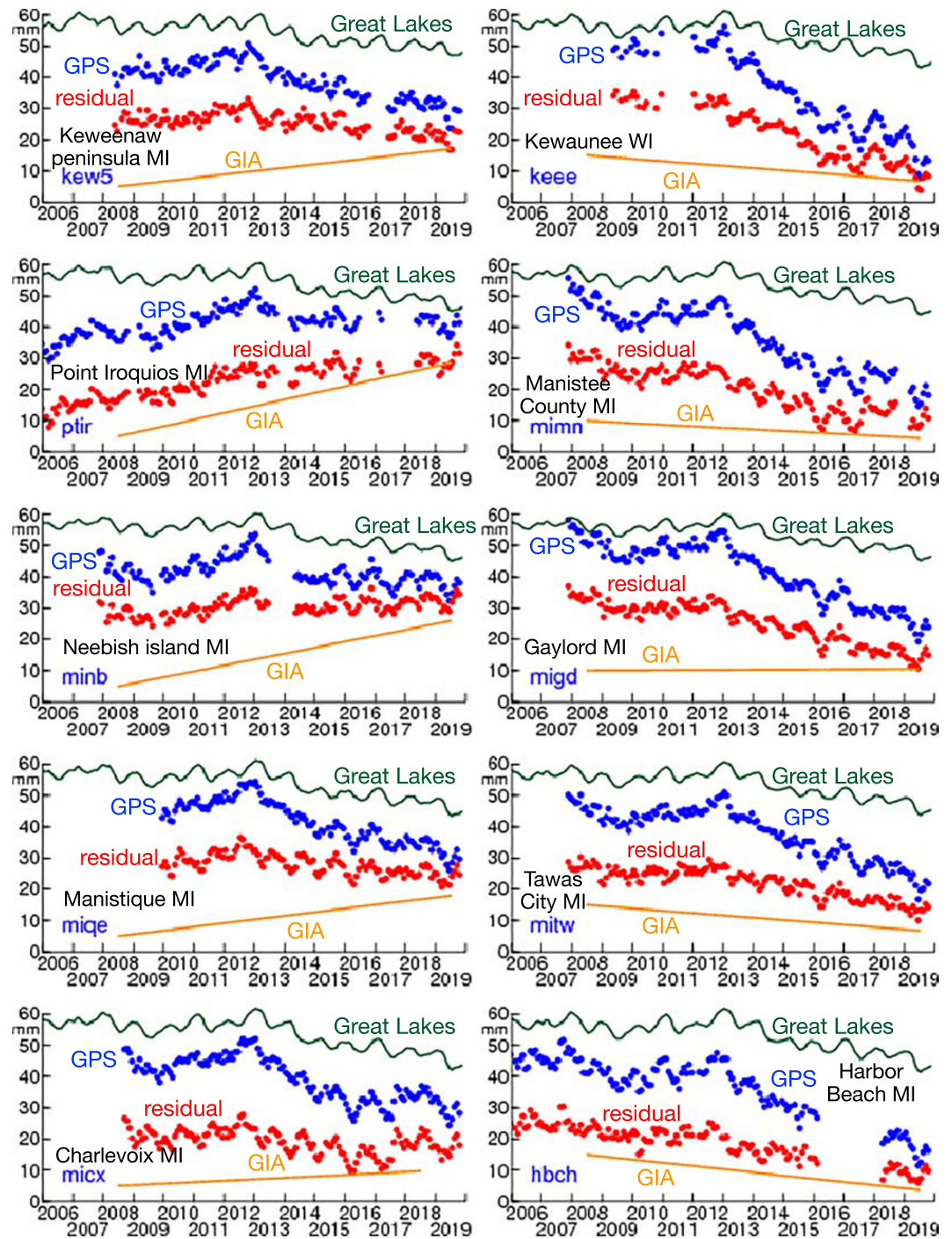


**Figure 4.** Vertical displacement each month of 10 GPS sites along or near the coast of Lake Michigan, Lake Huron, and Lake Superior. Elastic vertical displacement produced by changes in Great Lakes surface water (green) is removed from vertical displacement observed with GPS (blue) to estimate vertical displacement reflecting phenomena other than Great Lakes loading (red). Viscous vertical displacement produced by glacial isostatic adjustment (orange) is steady; the predictions of model ICE-6G\_D (VM5a) are plotted. The locations of the 10 GPS sites are shown in Figure 3 (site abbreviations in black text). See Figures S5–S7 for vertical displacements at 30 GPS sites near, respectively, Lake Superior, Lake Michigan, and Lake Huron.

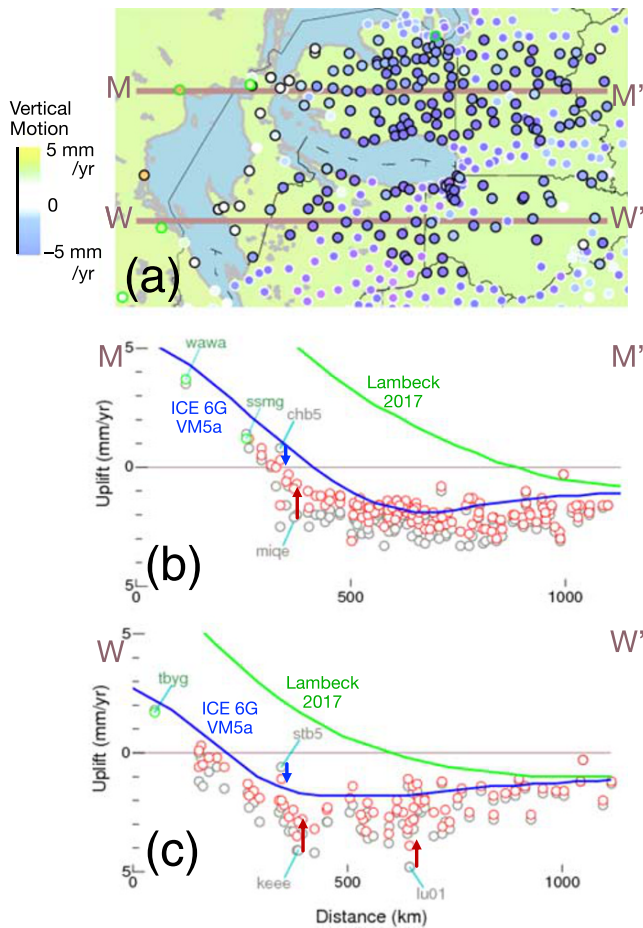


**Figure 5.** (a) GPS sites and two north-south profiles in the Lake Superior and Lake Michigan area (north on the map is toward left on the page). Continuous GPS sites within 150 km of either profile and with more than 8 years of data are circles with a black outline. Other continuous GPS sites are circles with a white outline. Campaign GPS sites from the Canadian Base Network are circles with a green outline. The color filling each circle designates the rate of vertical motion as given by the legend. (b and c) Rates of vertical motion observed with GPS (gray circles) are corrected for Great Lakes loading to deduce rates (red and green circles) caused primarily by glacial isostatic adjustment. Red circles are continuous GPS sites with more than 8 years of data. Green circles are campaign GPS sites from the Canadian Base Network. Correcting for Great Lakes loading increases the vertical rate of MIQE, KEEE, and LU01 (red arrows) and decreases the vertical rate of CHB5 and STB5 (blue arrows).

GPS vertical estimates at (MICX) Charlevoix, Michigan, decreases by 46% (from 4.6 to 2.5 mm). At most sites, correcting for elastic subsidence from 2013 to 2019 increases uplift over the 7 yr, making the evolution of positions from 2006 to 2019 more nearly a straight line. We present 10 examples of series corrections for GPS sites near Lakes Superior, Huron, and Michigan in Figure 4 and 10 series for each of Superior, Huron, and Michigan in Figures S5–S7, respectively.

Correcting time series of GPS sites near the Great Lakes for elastic surface water loading furthermore results in estimates of vertical motion that more nearly reflect solid Earth's viscous collapse of the forebulge of the late Pleistocene ice sheet (Figure S3). At most sites, GPS data start around 2007 and, because Great Lakes loading produces subsidence from 2013 to 2019, correcting for solid Earth's elastic response increases uplift (or reduces subsidence) at most GPS sites. For example, the subsidence rate of (KEEE) Kewaunee, Wisconsin, which subsided 12 mm from 2013 to 2019 in elastic response to increasing Great Lakes water, decreases from 4.2 to 3.0 mm/yr (Figures 4 and 5). Subsidence at (MIQE) Manistique, Michigan, which also subsided 12 mm from 2013 to 2019 due to Great Lakes loading, is reduced from 2.1 to 0.7 mm/yr. In contrast, the uplift rate of Cheybogan (CHB5), Michigan, which rose 12 mm from 1997 to 2001 in elastic response to decreasing Great Lakes water, decreases from 0.8 to 0.2 mm/yr. CHB5, with GPS data from 1995 to 2014, is more influenced by Great Lakes water loss from 1997 to 2001 than by Great Lakes water gain from 2013 to 2014. In total, correcting for Great Lakes loading reduces subsidence (or increases uplift) by more than 0.5 mm/yr at 148 GPS sites. Subsidence decreases by 1.0–2.2 mm/yr at 36 GPS sites. The decrease in subsidence rate is a maximum of 2.2 mm/yr at (LCUR) Little Current Lighthouse, near Manitoulin island (Ontario).

Correcting for solid Earth's elastic response to changes in Great Lakes surface water results in more accurate determination of the present-day rate of viscous collapse of the Laurentide ice sheet forebulge. Correcting for Great Lakes loading reduces subsidence rates in Michigan and Wisconsin by 1.0–2.2 mm/yr, bringing GPS estimates of rates of vertical motion closer to the predictions of glacial isostatic adjustment model ICE-6G\_D (VM5a) (Argus, Peltier et al., 2014; Peltier et al., 2015, 2018) (Figure 5). The mean residual of the GPS vertical rates relative to the ICE-6G\_D (VM5a) prediction is reduced from  $-0.86$  to  $-0.42$  mm/yr along Profile M-M' and from  $-1.41$  to  $-0.94$  mm/yr along Profile W-W'. The corrected GPS vertical rates are about 5 mm/yr more negative than glacial isostatic adjustment in the model of Lambeck et al. (2017).

cal rates are about 5 mm/yr more negative than glacial isostatic adjustment in the model of Lambeck et al. (2017).

### 3.4. Causes of Sinking of the Upper Midwest

Earth's surface in Michigan and Wisconsin is observed with GPS to be subsiding at 1–4 mm/yr (Figure 6). To investigate the cause of this subsidence, we next present a sequence of maps of vertical motion in eastern North America evaluating the contribution of different phenomena: oil pumping and groundwater withdrawal, postglacial rebound, and elastic Great Lakes loading. We find subsidence of the upper Midwest to be produced primarily by the collapse of the forebulge of Late Pleistocene/Early Holocene ice sheet and secondarily by solid Earth's elastic response to increased Great Lakes surface water.

GPS tightly constrains vertical land motion throughout North America (Argus & Peltier, 2010; Kreemer et al., 2018) (Figure 6a). We determine a map of the mean rate of vertical motion from about 2006 to 2019

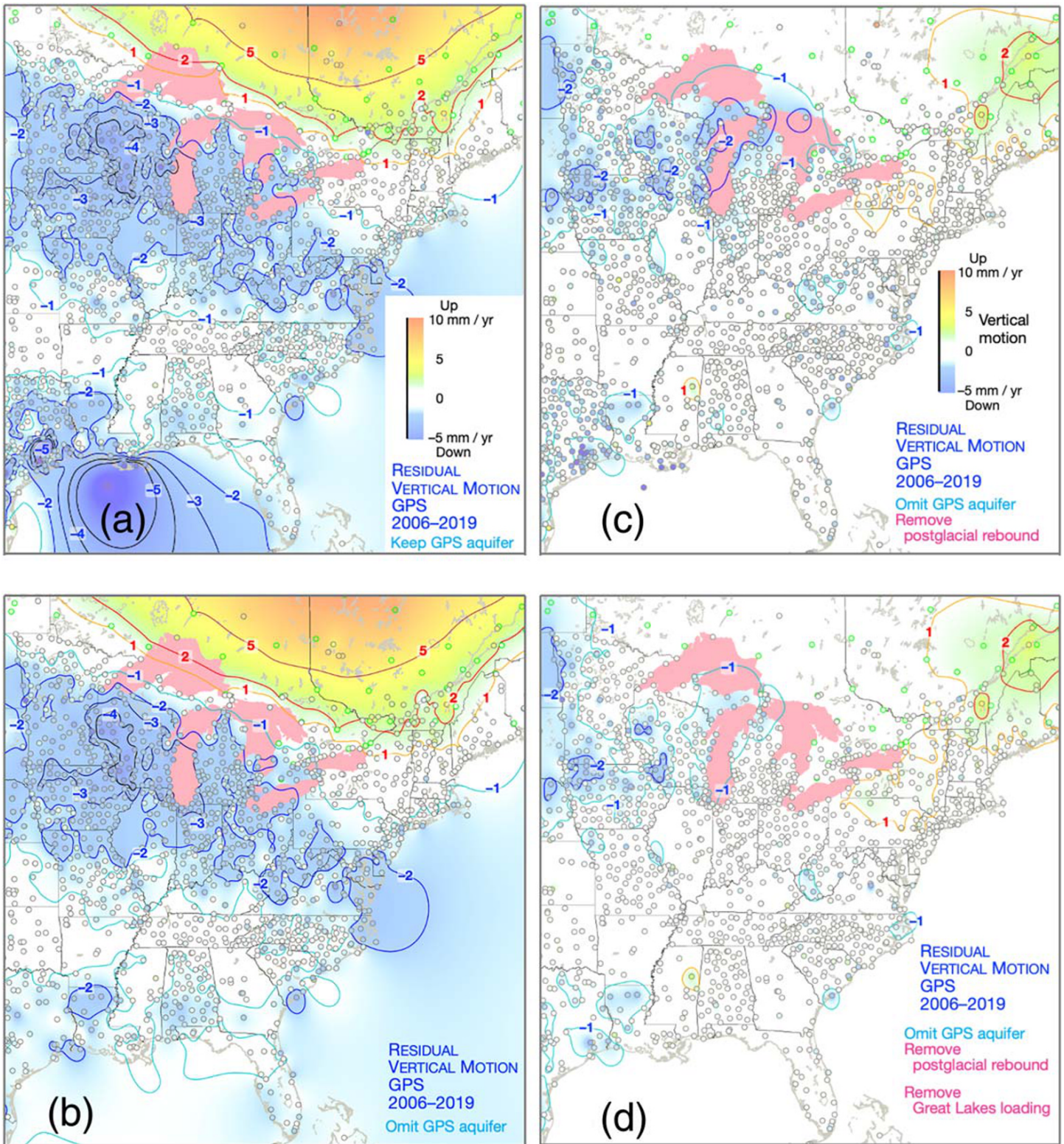


**Figure 6.** Rate of vertical motion in the eastern United States from about 2006 to 2019 (a) observed with GPS, (b) after discarding GPS sites that respond porously to groundwater withdrawal and oil pumping, (c) after further removing viscous glacial isostatic adjustment predicted by model ICE-6G\_D (VM5a), and (d) after further removing elastic Great Lakes loading. Vertical motion is relative to the mass center (CM) of Earth. Color gradations signify the rate of vertical motion, with blues depicting rates of subsidence faster than 1 mm/yr, yellows and reds depicting rates of uplift faster than 1 mm/yr, and white signifying nearly zero vertical motion between  $-1$  and  $1$  mm/yr. Contours are at 1, 2, and 5 mm/yr of uplift and at each 1 mm/yr interval of subsidence from  $-1$  to  $-5$  mm/yr.

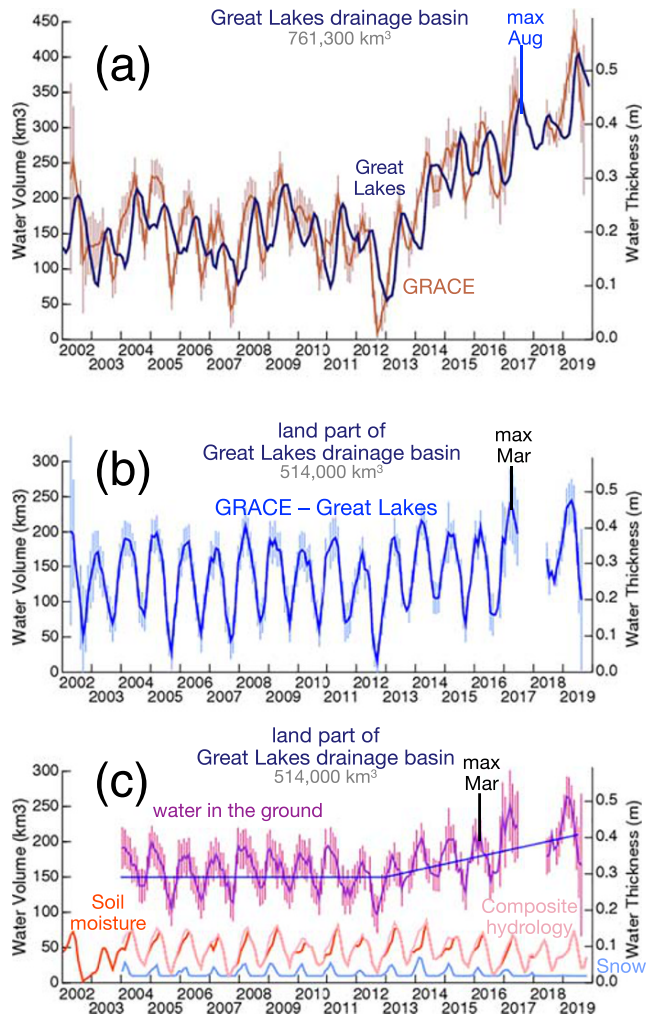


**Figure 7.** (a) Change in total water in the Great Lakes drainage basin estimated with GRACE (brown) reflects primarily change in surface water in the Great Lakes measured with water level gauges (navy blue). (b) Change in water on land in the drainage basin after removing Great Lakes surface water smeared by a Gaussian with a full width of 334 km (blue) is described by a uniform seasonal oscillation with a peak-to-peak amplitude of 100 km<sup>3</sup> and a maximum in March. (c) Change in water in the ground in the Great Lakes basin (violet) is inferred to be change in total water estimated with GRACE minus Great Lakes surface water minus a composite hydrology model (pink) consisting of snow in SNODAS (light blue) and soil moisture in NLDAS-Noah (orange). Change in water in the ground is described by a seasonal oscillation with a peak-to-peak amplitude of 60 km<sup>3</sup> with a maximum in February. Water in the ground is estimated to not change from 2004 to 2012 and to increase by a marginally significant  $50 \pm 50$  km<sup>3</sup> from 2013 to 2019. We calculate the values of water change in this figure assuming the Great Lakes area to extend 167 km from the lakes (see Figures S10 and S11).

by fitting a surface to 3,658 GPS rates of vertical motion in the United States and Canada. The velocity of Earth's center, the reference relative to which vertical motions are estimated, is constrained to  $\pm 0.5$  mm/yr ( $1\sigma$ ) (see section 4.3).

Roughly two thirds of the eastern United States are moving vertically at between 1 mm/yr of uplift and 2 mm/yr of subsidence (Figure 6a, white and light blue color gradations). There are two areas of fast subsidence: (1) an 800-km-long belt along the coast of southeast Texas and southern Louisiana is subsiding at 2–5 mm/yr (Karegar et al., 2015) and (2) a zone 500–1,000 km from north to south in the northern United States is subsiding at 2–4 mm/yr. This zone starts in Montana, cuts east across the Great Lakes region, and extends to the Atlantic coast near Maryland.

Part of the observed subsidence reflects management of water and oil resources. We next identify and eliminate the roughly 12% of GPS sites responding porously to groundwater fluctuations and oil pumping following the criteria of Argus et al., (2017, section 3.2). First, GPS sites that are subsiding quickly due to oil pumping along the Gulf coast are identified and omitted. Nine GPS sites in southern Louisiana and roughly 50 sites in southeastern Texas are observed to be subsiding faster than 2.5 mm/yr, reflecting the ground's porous response to oil pumping and groundwater withdrawal. Twelve GPS sites in Minnesota and nine sites in Wisconsin exhibit seasonal vertical oscillations reflecting porous response, including five sites in the Red Lake Peatland Scientific and Natural Area, Minnesota. Removing GPS sites responding to groundwater change and oil pumping eliminates the subsidence belt along the Gulf coast and slightly reduces subsidence in Wisconsin and Minnesota (Figure 6b).

The forebulge of Late Pleistocene/Early Holocene Laurentide ice sheet is presently predicted to be collapsing at 1–3 mm/yr in model ICE-6G\_D (VM5a) (Argus et al. 2014; Peltier et al., 2015, 2018) (Figure S3). Removing this glacial isostatic adjustment significantly reduces subsidence throughout the northern part of the eastern United States, leaving just 1–2 mm/yr of subsidence in Michigan, Wisconsin, Minnesota, and Iowa (Figure 6c).

Removing the effect of Great Lakes loading further reduces subsidence in most areas of the upper Midwest to just 0–1 mm/yr (Figure 6d). Roughly 90% of the eastern United States is moving vertically at between 1 mm/yr of uplift and –1 mm/yr of subsidence after glacial isostatic adjustment and Great Lakes loading are removed. There are two exceptions. Residual subsidence at 1–3 mm/yr occurs near the Minnesota-Dakotas border. There we postulate the true viscous collapse of the forebulge to be faster than in ICE-6G\_D (VM5a). Residual uplift of 1–3 mm/yr occurs near the Saint Lawrence River. There we believe the true viscous uplift to be faster than in ICE-6G\_D (VM5a).

Using InSAR and GPS data, Li et al. (2020) find the region between Lake Ontario, Lake Erie, and Lake Huron to have fallen 5–30 mm from 2013 to 2017. We maintain this subsidence to be primarily solid Earth's elastic response to unloading of Great Lakes water and secondarily the viscous collapse of the former Laurentide forebulge.

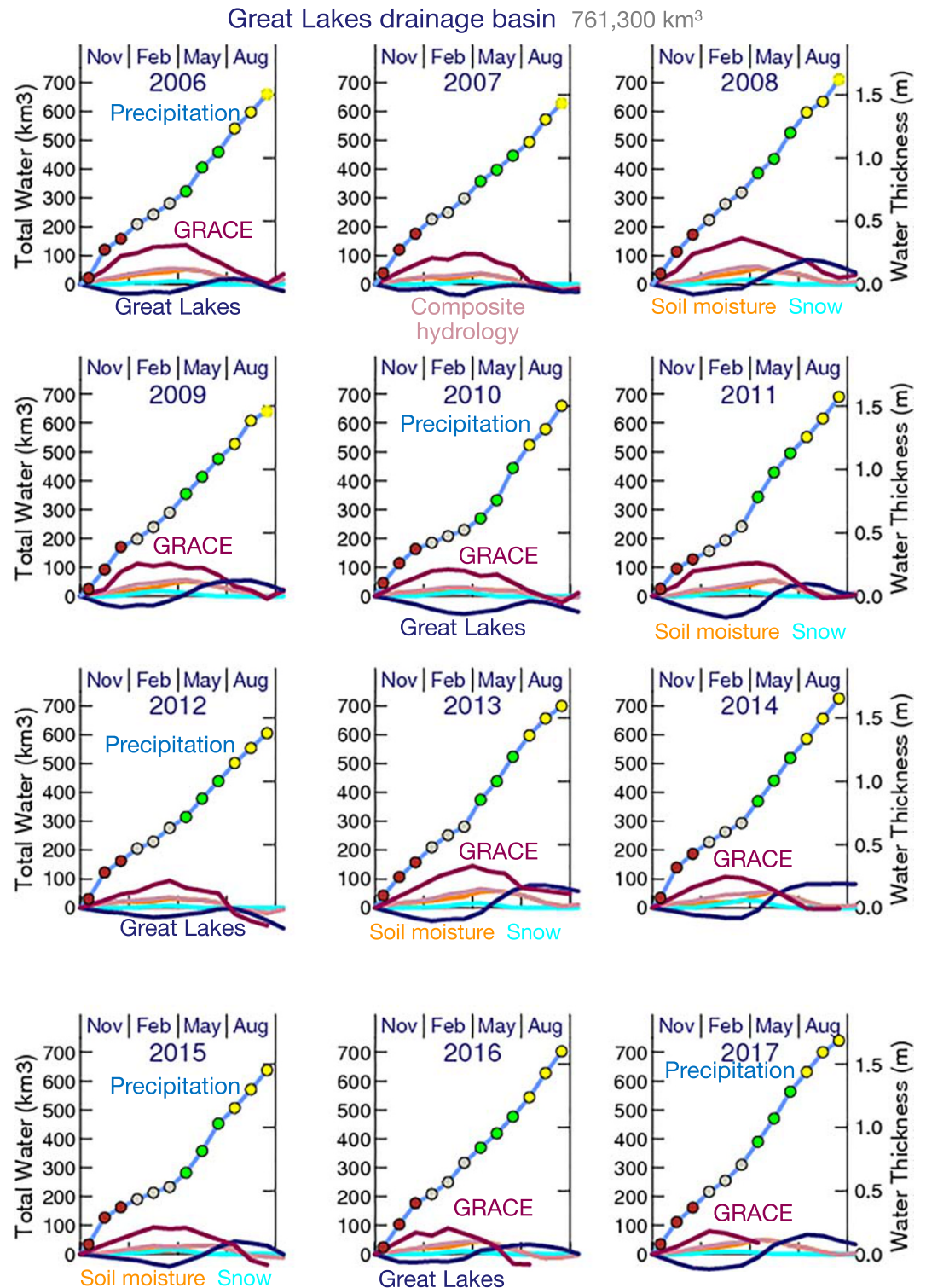


**Figure 8.** The time evolution of components of water storage in the Great Lakes drainage basin in each water year from 2006 to 2017. A water year starts 1 October and ends 30 September the following year. Precipitation (dots filled with different colors) accumulates steadily each year and total precipitation remains about the same from year to year. Great Lakes surface water (navy blue curve) is maximum each year around August, 3–6 months before water elsewhere in the drainage basin estimated from GRACE (maroon curve) is maximum. The composite hydrology model (pink curve) consists of snow water equivalent in SNODAS (cyan curve) and soil moisture in NLDAS-Noah (orange curve). Vertical axes at left are in cubic kilometers; vertical axes at right are in meters of equivalent water thickness.

### 3.5. Water Change in the Great Lakes Drainage Basin

#### 3.5.1. Total Water

Change in total water storage in the Great Lakes drainage basin reflects primarily change in surface water in the five Great Lakes. From 2002 to 2012, the total volume of water in the Great Lakes watershed is observed with GRACE to have remained about constant ( $-10 \text{ km}^3$ ); surface water volume in the Great Lakes measured with water level gauges has also remained about constant ( $-14 \text{ km}^3$ ) (Figure 7a). From 2013 to 2019, total water storage in the Great Lakes watershed is observed with GRACE to have increased by  $210 \text{ km}^3$ , slightly greater than the  $195 \text{ km}^3$  increase in Great Lakes surface water measured with water level gauges. However, as we shall show, total water change on land in the Great Lakes watershed observed with GRACE is about 6 months out of phase with surface water change in the five Great Lakes.

GRACE determines mass change at a spatial resolution of about 350 km, a distance slightly less than the 450-km altitude of the two GRACE satellites. Therefore, GRACE observes water change in the Great Lakes as a signal that is smeared out across a distance of about 350 km. Following Wahr et al. (1998), we model the mass change signal that GRACE would be expected to observe by applying a two-dimensional Gaussian distribution with a full width of 334 km (or three angular degrees) to the change in the Great Lakes water measured with water level gauges. We first apply the Gaussian distribution and next average the resulting values of smeared water change in each  $3^\circ \times 3^\circ$  mascon (in JPL's solution; Watkins et al., 2015; Wiese et al., 2016) (Figure S8). We find that a Gaussian distribution with a full width of 334 km well approximates gravity changes observed with GRACE (Figure S9). A Gaussian distribution with a full width of 222 km ( $2^\circ$ ) smears out Great Lakes water change across too narrow an area, whereas a Gaussian with a full width of 445 km ( $4^\circ$ ) smears out Great Lakes water change over too wide an area. In similar fashion, Chen et al. (2017) use a Gaussian distribution with a full width of 300 km to approximate the GRACE gravity signal produced by water change in the Caspian Sea measured by satellite altimetry.

#### 3.5.2. Water on Land

We thus estimate changes in total water on land in the Great Lakes watershed by removing the Gaussian-smoothed realization of Great lakes surface water change from the GRACE estimate of total mass change (Figures 7b and S12–S14). In the long term, we find that water on land in the Great Lakes watershed to have remained nearly constant from 2002 to 2012 and to have increased by  $35 \text{ km}^3$  from 2013 to 2019. In the seasons, we find water on land in the Great Lakes watershed to have increased each autumn and winter by an average of  $100 \text{ km}^3$  as snow accumulates on the ground and water infiltrates into the ground when evapotranspiration is low and to have decreased each spring and summer by an identical average of  $100 \text{ km}^3$  as snow melts and as water runoff passes through rivers into the Great Lakes when evapotranspiration is high. Water on land in the drainage basin reaches a maximum in March, 6 months before water in the Great Lakes attains a maximum in September. The seasonal oscillation in water on land has a peak-to-peak amplitude of  $100 \text{ km}^3$  with a maximum in March, twice as large but in phase with the  $50\text{-km}^3$  amplitude and March maximum in the composite hydrology model consisting of snow in SNODAS and soil moisture in NLDAS-Noah.

The changes in water on land in the Great Lakes drainage basin that we estimate are not very sensitive to the area that water is averaged over (Figures S10 and S11). We take GRACE water change calculated over an area extending 167 km (1.5 angular degrees) from the Great Lakes (Figure S10, tan outline) to be representative of change in the Great Lakes watershed because adopting JPL's  $3^\circ \times 3^\circ$  mascon solution distributes some water change associated with Great Lakes surface water change outside the true Great Lakes drainage basin (Figure S10, maroon outline). The values of water change that we calculate assuming an area extending 167 km from the Great Lakes ( $1,001,200 \text{ km}^2$ ) are intermediate between those calculated from the true Great Lakes watershed ( $761,300 \text{ km}^2$ ) and those calculated from an area consisting of ten  $3^\circ \times 3^\circ$  mascons ( $1,118,300 \text{ km}^2$ ) (Figure S10, green squares).

#### 3.5.3. Groundwater

We infer groundwater to be total water from GRACE minus the Gaussian-smoothed realization of Great Lakes water change minus the composite hydrology model consisting of soil moisture in NLDAS-Noah and snow in SNODAS. Hydrology models typically specify soil moisture in the top 0.5–2 m of the ground beneath Earth's surface; additional water may exist in the vadose zone, the unsaturated zone between Earth's surface and the groundwater table.

We find the seasonal oscillation of groundwater in the Great Lakes drainage basin to have a peak-to-peak amplitude of  $60 \text{ km}^3$  with a maximum around March 1. This  $60\text{-km}^3$  oscillation amounts to an average equivalent water thickness of  $0.12 \text{ m}$  over the land part of the Great Lakes watershed. We infer that groundwater (plus any water in the vadose zone) increases by an average of  $60 \text{ km}^3$  each autumn and winter and decreases by an identical average amount in the spring and summer.

Each autumn and winter, precipitation exceeds runoff plus evapotranspiration in the Great Lakes watershed, resulting in an increase in water storage on land (Figure 8). Precipitation is roughly uniform throughout the year. Each year water storage on land increases in the autumn and winter as snow accumulates when evapotranspiration is low and decreases in the spring and summer when snow melts and the resulting water runoff passes through rivers into the Great Lakes when evapotranspiration is high.

In the long term, groundwater in the Great Lakes drainage basin remained constant from 2004 to 2012. Groundwater then increased by  $50 \text{ km}^3$  from 2013 to 2019, amounting to an average of  $0.10 \text{ m}$  over the land part of the drainage basin. The  $50 \pm 50 \text{ km}^3$  increase from 2013 to 2019 is marginally significant. Half of the increase is attributable to a  $25 \text{ km}^3$  decrease in soil moisture in the NLDAS-Noah hydrology model. It is doubtful that soil moisture would decrease during heavy precipitation from 2013 to 2019, so that the groundwater increase might be instead  $25 \pm 50 \text{ km}^3$ . Any increase in groundwater in the drainage basin from 2013 to 2019 occurs in the southern part of the drainage basin and is associated with the large increase of water near the Mississippi River basin to the south (Figure S14).

We estimate groundwater to have changed by a mean of  $0.10 \pm 0.10\text{-m}$  water thickness over the land part of the Great Lakes drainage basin from 2013 to 2019. The face value estimate of  $0.10 \text{ m}$  is 10% of the rise of Great Lakes water levels, about  $1 \text{ m}$ . It is difficult to evaluate the meaning of the 1 to 10 ratio of groundwater gain to surface water gain. If the porosity of the sediment that the groundwater saturates is 5%, then an increase of  $0.10 \text{ m}$  in equivalent water thickness would result in an increase of  $2 \text{ m}$  ( $0.10 \text{ m}/0.05$ ) in the height of the water table. We suspect soil moisture has not decreased by an equivalent water thickness of  $0.05 \text{ m}$  from 2013 to 2019 as in the hydrology model. If soil moisture were instead assumed to have remained constant from 2013 to 2019, then the rise in equivalent water thickness would be  $0.05 \text{ m}$ , and the hypothetical increase in the height of the water table would be  $1 \text{ m}$  given a sediment porosity of 5%.

About half of Michigan and eastern Wisconsin is between 0 and  $85 \text{ m}$  above the levels of the Lake Michigan, Lake Huron, and Lake Superior. The water table is believed to be in most places in Michigan and eastern Wisconsin within  $5 \text{ m}$  of Earth's surface (<https://www.egr.msu.edu/igw/GWIM%20Figure%20Webpage/>) (Figure 7). Thus, the water table on land is in most places several tens of meters above the Great Lakes water level. There may be a mounding effect: Water in Michigan, eastern Wisconsin, and southern Ontario flows downslope into the Great Lakes. Part of a groundwater increase may be adjacent to the Great Lakes where the water table is at or near the same level as the Great Lakes water levels and has risen with the Great Lakes, although this area is a small fraction of the Great Lakes drainage basin. Groundwater may increase in deep aquifers not near Earth's surface. Water in the many lakes in Michigan, Wisconsin, and Ontario's glacial terrain may take up a water increase.

### 3.6. Seasonal Oscillations in Vertical Displacement Produced by Changes in Water on Land

GPS measurements of solid Earth's elastic response further constrain how seasonal fluctuations in water on land vary across the Great Lakes drainage basin. We first compare seasonal oscillations in vertical position observed with GPS, those produced by Great Lakes loading, and those predicted by water change as observed by GRACE in a phasor diagram (Figure S15). Following the strategy we have established, we next remove from the GPS and the GRACE estimates the effect of changes in Great Lakes surface water and thus evaluate seasonal vertical positions inferred to be produced by changes in water on land (Figures S16 and S17). In the Lower Peninsula of Michigan, the seasonal oscillation in vertical position inferred from GPS to reflect changes in water on land has a peak-to-peak amplitude of roughly  $4 \text{ mm}$  with a maximum in August or September, 6 months after water on land is maximum in March or April (Figure S17a, blue arrows). This maximum is about the same size but 1 month earlier than the seasonal vertical oscillation inferred from GRACE (maroon arrows), has an amplitude of  $6.5 \text{ mm}$  with a maximum vertical position in September. In Wisconsin, the seasonal oscillation in vertical position inferred from GPS has a peak-to-peak amplitude of  $4 \text{ mm}$  with a maximum in November to December (Figure S17b, blue arrows), suggesting water on

land to be maximum in May to June. This maximum is slightly smaller than and 1 to 2 months later than that observed with GRACE, which has an amplitude of 6 mm with a maximum vertical position in September (maroon arrows). In southern Ontario, few GPS sites exist to support or refute the inference from GRACE that water on land fluctuates each year by about 0.20 m, twice as large as in the composite hydrology model (Figure S17).

## 4. Discussion

### 4.1. This Study Versus Huang et al. (2012)

Following Huang et al. (2012), we take groundwater change to be total water estimated using GRACE minus Great Lakes surface water minus snow and soil moisture in our composite hydrology model. In the long term, we estimate groundwater to have hardly changed ( $-1 \text{ km}^3$ ) from 2004 to 2009, whereas Huang et al. (2012, abstract) find groundwater to have decreased significantly ( $-45 \text{ km}^3$ ) from 2002 to 2009. Using 7 yr of data that were unavailable to Huang et al. (2012), we estimate groundwater to have increased by a marginally significant  $50 \pm 50 \text{ km}^3$  from 2013 to 2019. In the seasons, we find groundwater to increase  $60 \text{ km}^3$  in the winter and fall and decrease by a roughly equivalent amount in the spring and summer. We find groundwater on land to reach a maximum in March, 6 months before Great Lakes surface water peaks in September. In contrast, Huang et al. (2012, Figure 16) find groundwater to attain a maximum around September if the Water Gap Hydrology model is removed, and groundwater to have incoherent seasonal fluctuations if the NLDAS-Noah model or a mean of four GLDAS models is removed. Thus, we find the seasonal fluctuation in groundwater to be quite different than in Huang et al. (2012).

### 4.2. Thermal Expansion of Great Lakes Surface Water

Great Lakes water levels rise in thermal expansion each summer by roughly 0.040 m (Huang et al., 2012, Figure 2), slightly altering the value of water volume change calculated from the water level gauge data. Water volume in the Great Lakes as a function of temperature is specified by

$$1 - 6.427 \times 10^{-5} T + 8.5053 \times 10^{-6} T^2 - 6.79 \times 10^{-8} T^3$$

where  $T$  is temperature in  $^{\circ}\text{C}$  (Meredith, 1975, see also [https://www.engineeringtoolbox.com/water-density-specific-weight-d\\_595.html](https://www.engineeringtoolbox.com/water-density-specific-weight-d_595.html)). Water is most dense at  $4^{\circ}\text{C}$ . The density of Great Lakes water is nearly constant (within 0.01%) for the 9 months of the year when the temperature is at  $0^{\circ}\text{C}$  to  $8^{\circ}\text{C}$ . The top 25 m of Great Lakes water warms to roughly  $20^{\circ}\text{C}$  in the summer months of July, August, and September, increasing the volume of the top 25 m of water by 0.16%, resulting in a 0.040-m increase in water level (14% of the seasonal oscillation in Great Lakes water level of 0.291 m). Accounting for thermal expansion would reduce the seasonal fluctuation in equivalent water in the Great Lakes watershed in August by roughly  $10 \text{ km}^3$  (0.040-m Great Lakes water level increase  $\times$   $247,300\text{-km}^2$  Great Lakes area).

The calculation of the effect of thermal expansion depends strongly on the temperature that the top 25 m of water is assumed to attain in August, and the temperature-depth profile is not well known throughout the Great Lakes. For example, if we were to take the mean summer temperature in the top 25 m to be  $16^{\circ}\text{C}$  (as opposed to  $20^{\circ}\text{C}$ ), we would calculate the volume of the top 25 m to increase by 0.08%, producing a 0.020-m increase in water level. Accounting for thermal expansion would then reduce equivalent water volume in the Great Lakes watershed in August by just  $5 \text{ km}^3$  (as opposed to  $10 \text{ km}^3$ ).

In summary, our estimate of the seasonal fluctuation on land in the Great Lakes watershed would be reduced from 60 to  $50 \text{ km}^3$  (assume a  $20^{\circ}\text{C}$  maximum temperature) or  $55 \text{ km}^3$  (assuming a  $16^{\circ}$  maximum temperature) if we were to account for thermal expansion of the Great Lakes.

### 4.3. Uncertainty in the Velocity of Earth's Center

GPS tightly constrains the rate of vertical motion of Earth's surface throughout the United States. The uncertainty in the velocity of Earth's center, the reference relative to which vertical motion is estimated, is about a half millimeter/year ( $1\sigma$ ). Vertical motions are standardly estimated relative to the CM of the solid Earth and its fluid envelope, consisting of the atmosphere, oceans, and ice sheets. For example, estimates of vertical motion in ITRF2014 (Altamimi et al., 2016) are relative to CM. The velocity of Earth's surface relative to CM is estimated using satellite laser ranging (SLR) measurements to LAGEOS and is constrained to

$\pm 0.5$  mm/yr ( $1\sigma$ ). Using data decimation and spectral analysis, Argus (2012) estimates 95% confidence limits in the  $X$ ,  $Y$ , and  $Z$  directions to be  $\pm 0.4$ ,  $\pm 0.4$ , and  $\pm 0.9$  mm/yr, respectively. Using similar techniques but 6 yr more SLR data, Riddell et al. (2017) estimate the 95% confidence limits in  $X$ ,  $Y$ , and  $Z$  to be  $\pm 0.25$ ,  $\pm 0.33$ , and  $\pm 0.65$  mm/yr.

## 5. Conclusions

Great Lakes surface water rose 0.7–1.5 m from 2013 to 2019, increasing surface water volume by 285 km<sup>3</sup>. The floor of the Great Lakes fell 8–23 mm, and the adjacent land in Michigan, Wisconsin, southern Ontario, Illinois, Indiana, and Ohio fell 3–14 mm.

Solid Earth's surface in Wisconsin and Michigan fell at 1–4 mm/yr from 2006 to 2019. This sinking was produced primarily by viscous collapse of the forebulge of the Late Pleistocene Laurentide ice sheet and secondarily by solid Earth's elastic response to increased Great Lakes surface water.

Seasonal water storage on land in the Great Lakes basin is inferred from GRACE and GPS to be maximum in March and to be twice as large as that in a hydrology model. The seasonal oscillation in water in the ground is 60 km<sup>3</sup> (0.12 m averaged over the land part of the Great Lakes drainage basin), about equal to the seasonal oscillation in snow and soil moisture in a hydrology model.

We look forward to hydrologists integrating our inferences of water change inferred from GRACE with analyses of groundwater well levels and land surface models.

## Data Availability Statement

GPS position-time series are available at the Nevada Geodetic Laboratory (at [http://geodesy.unr.edu/gps\\_timeseries](http://geodesy.unr.edu/gps_timeseries)). GRACE water-time series (JPL's mascon solution, Release 6, Version 2) are available online (at <https://podaac-tools.jpl.nasa.gov/drive/files/allData/tellus/L3/mascon/RL06/JPL/v02>). The ICE 6G D/VM5a model of postglacial rebound is available online (at <http://www.atmosph.physics.utoronto.ca/~peltier/data.php>).

## Acknowledgments

We are grateful for many institutions for archiving and acquiring GPS data: UNAVCO, SOPAC, CDDIS, the Plate Boundary Observatory, and the National Geodetic Survey. We are grateful to Paul Ries (JPL) and JPL's GPS team for determining the GPS satellite orbits and clocks that are available online (at [https://sideshow.jpl.nasa.gov/JPL\\_GPS\\_Products/Final](https://sideshow.jpl.nasa.gov/JPL_GPS_Products/Final)). Michael Craymer and Joe Henton expertly acquired campaign measurements at 140 campaign GPS sites in the Canadian Base Network. Anthony Purcell (at Australian National University) provided the predictions of the postglacial rebound model of Lambeck et al. (2017). Lauren Fry (U.S. Army Corps of Engineers) provided instruction on data access to Great Lakes water levels and information on the water balance in the Great Lakes drainage basin. We are grateful to Nicola D'Agostino and Andrew Gronewold for their careful reviews of the manuscript. This project was funded by NASA NNH14ZDA001N-GNSS, NNH15ZDA001N-GRACE, and 80NSSC19K1044-ESI. Argus and Wiese's part of this research was performed at Jet Propulsion Laboratory, California Institute of Technology, under contract with NASA.

## References

- Adusumilli, S., Borsa, A. A., Fish, M. A., McMillan, H. K., & Silverii, F. (2019). A decade of water storage changes across the contiguous United States from GPS and satellite gravity. *Geophysical Research Letters*, *46*, 13006–13015. <https://doi.org/10.1029/2019GL085370>
- Agnew, D. C. (2013). SPOTL: Some programs for ocean-tide loading, Scripps Institution of Oceanography Technical Report, La Jolla.
- Altamimi, Z., Rebischung, P., Métivier, L., & Collilieux, X. (2016). ITRF2014: A new release of the International Terrestrial Reference Frame modeling nonlinear station motions. *Journal of Geophysical Research: Solid Earth*, *121*, 6109–6131. <https://doi.org/10.1002/2016JB013098>
- Argus, D. F. (2012). Uncertainty in the velocity between the mass center and surface of Earth. *Journal of Geophysical Research*, *117*, B10405. <https://doi.org/10.1029/2012JB009196>
- Argus, D. F., Fu, Y., & Landerer, F. W. (2014). Seasonal variation in total water storage in California inferred from GPS observations of vertical land motion. *Geophysical Research Letters*, *41*, 1971–1980. <https://doi.org/10.1002/2014GL059570>
- Argus, D. F., Gordon, R. G., Heflin, M. B., Ma, C., Eanes, R. J., Willis, P., et al. (2010). The angular velocities of the plates and the velocity of Earth's center from space geodesy. *Geophysical Journal International*, *180*(3), 913–960. <https://doi.org/10.1111/j.1365-246X.2009.04463.x>
- Argus, D. F., Landerer, F. W., Wiese, D. N., Martens, H. R., Fu, Y., Famiglietti, J. S., et al. (2017). Sustained water loss in California's mountain ranges during severe drought from 2012 to 2015 inferred from GPS. *Journal Geophysical Research Solid Earth*, *122*, 10,559–10,585. <https://doi.org/10.1002/2017JB014424>
- Argus, D. F., & Peltier, W. R. (2010). Constraining models of postglacial rebound using space geodesy: a detailed assessment of model ICE-5G (VM2) and its relatives. *Geophysical Journal International*, *181*. <https://doi.org/10.1111/j.1365-246X.2010.04562.x>
- Argus, D. F., Peltier, W. R., Drummond, R., & Moore, A. W. (2014). The Antarctica component of postglacial rebound model ICE-6G\_C (VM5a) based on GPS positioning, exposure age dating of ice thicknesses, and relative sea level histories. *Geophysical Journal International*, *198*(1), 537–563. <https://doi.org/10.1093/gji/ggu140>
- Blewitt, G., Hammond, W. C., & Kreemer, C. (2018). Harnessing the GPS data explosion for interdisciplinary science. *Eos*, *99*. <https://doi.org/10.1029/2018EO104623> Published on 24 September 2018
- Blewitt, G., Kreemer, C., Hammond, W. C., & Argus, D. F. (2019). Improved GPS position time series spanning up to 25 years for over 18,000 stations resulting from IGS Repro 3 products, JPL's GipsyX software, and more advanced modeling techniques. Abstract G12A-04, Fall 2019 American Geophysical Union, San Francisco
- Boehm, J., Werl, B., & Schuh, H. (2006). Troposphere mapping functions for GPS and very long baseline interferometry from European Centre for Medium-Range Weather Forecasts operational analysis data. *Journal of Geophysical Research*, *111*, B02406. <https://doi.org/10.1029/2005JB003629>
- Borsa, A. A., Agnew, D. C., & Cayan, D. R. (2014). Ongoing drought-induced uplift of the western United States. *Science*, *345*(6204), 1587–1590. <https://doi.org/10.1126/science.1260279>
- Chen, J. L., Pekker, T., Wilson, C. R., Tapley, B. D., Kostianoy, A. G., Cretaux, J.-F., & Safarov, E. S. (2017). Long-term Caspian Sea level change. *Geophysical Research Letters*, *44*, 6993–7001. <https://doi.org/10.1002/2017GL073958>

- D'Urso, M. G., & Marmo, F. (2013). On a generalized Love's problem. *Computers and Geosciences*, *61*, 144–151. <https://doi.org/10.1016/j.cageo.2013.09.002>
- Dahle, C., Murböck, M., Fletchner, F., Dobslaw, H., Michalak, G., Neumayer, K. H., et al. (2019). The GFZ GRACE RL06 monthly gravity field series: Processing details and quality assessment. *Remote Sensing*, *11*(18), 2116. <https://doi.org/10.33390/rs11182116>
- Dempsey, D., Elder, J., & Scavia, D. (2008). Great Lakes restoration and the threat of global warming, Healing Our Waters-Great Lakes Coalition. [https://www.nwf.org/%20-/media/PDFs/Water/200711\\_ClimateChangeandGreatLakes\\_Report](https://www.nwf.org/%20-/media/PDFs/Water/200711_ClimateChangeandGreatLakes_Report)
- Dill, R., & Dobslaw, H. (2013). Numerical simulations of global-scale high-resolution hydrological crustal deformations. *Journal of Geophysical Research: Solid Earth*, *118*, 5008–5017. <https://doi.org/10.1002/jgrb.50353>
- Dziewonski, A. M., & Anderson, D. L. (1981). Preliminary reference Earth model. *Physics of the Earth and Planetary Interiors*, *25*(4), 297–356. [https://doi.org/10.1016/0031-9201\(81\)90046-7](https://doi.org/10.1016/0031-9201(81)90046-7)
- Enzlinger, T. L., Small, E. E., & Borsa, A. A. (2019). Subsurface water dominates Sierra Nevada seasonal hydrologic storage. *Geophysical Research Letters*, *46*, 11993–12001. <https://doi.org/10.1029/2019GL084589>
- Farrell, W. E. (1972). Deformation of the Earth by surface loads. *Reviews of Geophysics*, *10*(3), 761–797. <https://doi.org/10.1029/RG010i003p00761>
- Fu, Y., Argus, D. F., & Landerer, F. W. (2015). GPS as an independent measurement to estimate terrestrial water storage variations in Washington and Oregon. *Journal of Geophysical Research: Solid Earth*, *120*, 552–566. <https://doi.org/10.1002/2014JB011415>
- Gronewold, A. D., Bruxer, J., Durnford, D., Smith, J. P., Clites, A. H., Seglenieks, F., et al. (2016). Hydrological drivers of record-setting water level rise on Earth's largest lake system. *Water Resources Research*, *52*, 4026–4042. <https://doi.org/10.1002/2015WR018209>
- Gronewold, A. D., Fortin, V., Caldwell, R., & Noel, J. (2018). Resolving hydrometeorological data discontinuities along an international border. *Bulletin of the American Meteorological Society*, *99*(5), 899–910. <https://doi.org/10.1175/BAMS-D-16-0060.1>
- Gronewold, A. D., Fortin, V., Lofgren, B. M., Clites, A. H., Stow, C. A., & Quinn, F. H. (2013). Coasts, water levels, and climate change: A Great Lakes perspective. *Climatic Change*, *120*(4), 697–711. <https://doi.org/10.1007/s10584-013-0840-2>
- Huang, J., Halpenny, J., van der Wal, W., Klatt, C., James, T. S., & Rivera, A. (2012). Detectability of groundwater storage change within the Great Lakes Water Basin using GRACE. *Journal of Geophysical Research*, *117*, B08401. <https://doi.org/10.1029/2011JB008876>
- Jia, Y., Shum, C. K., Chu, P., & Forootan, E. (2018). Monitoring water level variations over the Great Lakes using contemporary satellite geodetic observations. Abstract H31K–2074, Fall 2018 American Geophysical Union Meeting, Washington, D.C.
- Karegar, M. A., Dixon, T. H., & Malservisi, R. (2015). A three-dimensional surface velocity field for the Mississippi Delta: Implications for coastal restoration and flood potential. *Geology*, *43*(6), 519–522. <https://doi.org/10.1130/G36598.1>
- Kling, G. W., Hayhoe, K., Johnson, L. B., Magnuson, J. J., Polasky, S., Robinson, S. K., et al. (2003). *Confronting climate change in the Great Lakes Region: Impacts on our communities and ecosystems*. Cambridge, Massachusetts: Union of Concerned Scientists. and Ecological Society of America, Washington, D.C.
- Kreemer, C., Hammond, W. C., & Blewitt, G. (2018). A robust estimation of the 3-D intraplate deformation of the North American plate from GPS. *Journal of Geophysical Research: Solid Earth*, *123*, 4388–4412. <https://doi.org/10.1029/2017JB015257>
- Lambeck, K., Purcell, A., & Zhao, S. (2017). The North America Late Wisconsin ice sheet ice sheet and mantle viscosity from glacial rebound analyses. *Quaternary Science Reviews*, *158*, 172–210. <https://doi.org/10.1016/j.quascirev.2016.11.033>
- Li, J., Wang, S., Michel, C., & Russell, H. A. J. (2020). Surface deformation observed by InSAR shows connections with water storage change in southern Ontario. *Journal of Hydrology: Regional Studies*, *27*, 100661. <https://doi.org/10.1016/j.ejrh.2019.100661>
- Luthcke, S. B., Sabaka, T. J., Loomis, B. D., Arendt, A. A., McCarthy, J. J., & Camp, J. (2013). Antarctica, Greenland and Gulf of Alaska land-ice evolution from an iterated GRACE global mascon solution. *Journal of Glaciology*, *59*(216), 613–631. <https://doi.org/10.3189/2013JG12J147>
- Mainville, A., & Craymer, M. R. (2005). Present-day tilting of the Great Lakes region based on water level gauges. *Geological Society of America Bulletin*, *117*(7), 1070–1080. <https://doi.org/10.1130/B25392>
- Martens, H. R., Rivera, L., & Simons, M. (2019). LoadDef: A Python-based toolkit to model elastic deformation caused by surface mass loading on spherically symmetric bodies. *Earth and Space Science*, *6*, 311–323. <https://doi.org/10.1029/2018EA000462>
- Meredith, D. D. (1975). Temperature effects on Great Lakes water balance studies. *Water Resources Bulletin*, *11*(1), 60–68. <https://doi.org/10.1111/j.1752-1688.1975.tb00660.x>
- Mitchell, K. E., Lohmann, D., Houser, P. R., Wood, E. F., Schaake, J. C., Robock, A., et al. (2004). The multi-institution North American Land Data Assimilation System (NLDAS): Utilizing multiple GCM products and partners in a continental distributed hydrological modeling system. *Journal of Geophysical Research*, *109*, D07S90. <https://doi.org/10.1029/2003JD003823>
- National Operational Hydrologic Remote Sensing Center (2004). *Snow Data Assimilation System (SNODAS) data products at NSIDC*. Boulder, CO: National Snow and Ice Data Center. <https://doi.org/10.7265/N5TB14TC>
- National Snow and Ice Data Center (2019). Retrieved from [http://nsidc.org/data/docs/noaa/g02158\\_snodas\\_snow\\_cover\\_model/](http://nsidc.org/data/docs/noaa/g02158_snodas_snow_cover_model/)
- Pan, M., Sheffield, J., Wood, E. F., Mitchell, K. E., Houser, P. R., Schaake, J. C., et al. (2003). Snow process modeling in the North American Land Data Assimilation System (NLDAS): 2. Evaluation of model simulated snow water equivalent. *Journal of Geophysical Research*, *108*(D22), 8850. <https://doi.org/10.1029/2003JD003994>
- Peltier, W. R., Argus, D. F., & Drummond, R. (2015). Space geodesy constrains ice age terminal deglaciation: The global ICE-6G\_C (VM5a) model. *Journal of Geophysical Research: Solid Earth*, *120*, 450–487. <https://doi.org/10.1002/2014JB011176>
- Peltier, W. R., Argus, D. F., & Drummond, R. (2018). Comment on “An assessment of ICE-6G\_C (VM5a) glacial isostatic adjustment model” by Purcell et al. *Journal of Geophysical Research: Solid Earth*, *123*, 2029–2032. <https://doi.org/10.1002/2016JB013844>
- Reager, J. T., Thomas, B. F., & Famiglietti, J. S. (2014). River basin flood potential inferred using GRACE gravity observations at several months lead time. *Nature Geoscience*, *7*(8), 588–592. <https://doi.org/10.1038/ngeo2203>
- Reischung, P., Altamimi, Z., Ray, J., & Garayt, B. (2016). The IGS contribution to ITRF2014. *Journal of Geodesy*, *90*(7), 611–630. <https://doi.org/10.1007/s00190-016-0897-6>
- Riddell, A. R., King, M. A., Watson, C. S., Sun, Y., Riva, R. E. M., & Rietbroek, R. (2017). Uncertainty in geocenter estimates in the context of ITRF2014. *Journal of Geophysical Research: Solid Earth*, *122*, 4020–4032. <https://doi.org/10.1029/2016JB013698>
- Roy, K., & Peltier, W. R. (2017). Space-geodetic and water level gauge constraints on continental uplift and tilting over North America: Regional convergence of the ICE-6G C (VM5a/VM6) models. *Geophysical Journal International*, *210*(2), 1115–1142. <https://doi.org/10.1093/gji/ggx156>
- Save, H., Bettadpur, S., & Tapley, B. D. (2016). High resolution CSR GRACE RL05 Mascons. *Journal of Geophysical Research: Solid Earth*, *121*, 7547–7569. <https://doi.org/10.1002/2016JB013007>

- Scanlon, B. R., Zhang, Z., Save, H., Sun, A. Y., Schmied, H. M., van Beek, L. P. H., et al. (2018). Global models underestimate large decadal declining and rising water storage trends relative to GRACE satellite data. *Proceedings of the National Academy of Sciences*, *115*(6), E1080–E1089. <https://doi.org/10.1073/pnas.1704665115>
- Wahr, J., Khan, S. A., van Dam, T., Liu, L., van Angelen, J. H., van den Broeke, M. R., & Meertens, C. M. (2013). The use of GPS horizontals for loading studies, with applications to northern California and southeast Greenland. *Journal of Geophysical Research: Solid Earth*, *118*, 1795–1806. <https://doi.org/10.1002/jgrb.50104>
- Wahr, J., Molenaar, M., & Bryan, F. (1998). Time variability of the Earth's gravity field: Hydrological and oceanic effects and their possible detection using GRACE. *Journal of Geophysical Research*, *103*(B12), 30205–30229. <https://doi.org/10.1029/98JB02844>
- Wang, H., Xiang, L., Jia, L., Jiang, L., Wang, Z., Hu, B., & Gao, P. (2012). Load Love numbers and Green's functions for elastic Earth models PREM, iasp91, ak135, and modified models with refined crustal structure from crust 2.0. *Computational Geosciences*, *49*, 190–199. <https://doi.org/10.1016/j.cageo.2012.06.022>
- Watkins, M. M., Wiese, D. N., Yuan, D.-N., Boening, C., & Landerer, F. W. (2015). Improved methods for observing Earth's time variable mass distribution with GRACE using spherical cap mascons. *Journal of Geophysical Research: Solid Earth*, *120*, 2648–2671. <https://doi.org/10.1002/2014JB011547>
- Wiese, D. N., Landerer, F. W., & Watkins, M. M. (2016). Quantifying and reducing leakage errors in the JPL RL05M GRACE mascon solution. *Water Resources Research*, *52*, 7490–7502. <https://doi.org/10.1002/2016WR019344>

### References From the Supporting Information

- Argus, D. F. (2007). Defining the translational velocity of the reference frame of Earth. *Geophysical Journal International*, *169*(3), 830–838. <https://doi.org/10.1111/j.1365-246X.2007.03344.x>
- Bertiger, W., Bar-Sever, Y., Dorsey, A., Haines, B., Harvey, N., Hemberger, D., et al. (2020). GipsyX/RTGx, a new tool set for space geodetic operations and research. *Advances in Space Research*, *66*(3), 469–489. <https://doi.org/10.1016/j.asr.2020.04.015>
- Boehm, J., Werl, B., & Schuh, H. (2006). Troposphere mapping functions for GPS and very long baseline interferometry from European Centre for Medium-Range Weather Forecasts operational analysis data. *Journal of Geophysical Research*, *111*, B02406. <https://doi.org/10.1029/2005JB003629>
- Dee, D. P., Uppala, S. M., Simmons, A. J., Berrisford, P., Poli, P., Kobayashi, S., et al. (2011). The ERA-Interim reanalysis: Configuration and performance of the data assimilation system. *Quarterly Journal of the Royal Meteorological Society*, *137*(656), 553–597. <https://doi.org/10.1002/qj.828>
- Dobslaw, H., Bergmann-Wolf, I., Dill, R., Poropat, L., Thomas, M., Dahle, C., et al. (2017). A new high-resolution model of non-tidal atmosphere and ocean mass variability for de-aliasing of satellite gravity observations: AOD1B RL06. *Geophysical Journal International*, *211*(1), 263–269. <https://doi.org/10.1093/gji/ggx302>
- Rebischung, P., & Schmid, R. (2016). IGS14/igs14.atx: A new framework for the IGS products. Abstract G41A–0998, Fall 2016 American Geophysical Union, San Francisco
- Vacchi, M., Engelhart, S. E., Nikitina, D., Ashe, E. L., Peltier, W. R., Roy, K., et al. (2018). Postglacial relative sea-level histories along the eastern Canadian coastline. *Quaternary Science Reviews*, *201*, 124–146. <https://doi.org/10.1016/j.quascirev.2018.09.043>
- Zumberge, J. F., Heflin, M. B., Jefferson, D. C., Watkins, M. M., & Webb, F. H. (1997). Precise point positioning for the efficient and robust analysis of GPS data from large networks. *Journal of Geophysical Research*, *102*(B3), 5005–5017. <https://doi.org/10.1029/96JB03860>